ACS OMEGA

http://pubs.acs.org/journal/acsodf

Article

Inhibition Mechanism of Methicillin-Resistant *Staphylococcus aureus* by Zinc Oxide Nanorods via Suppresses Penicillin-Binding Protein 2a

Amr Hassan,* Fawziah A. AL-Salmi, Muneera A. Saleh, Jean-Marc Sabatier, Fuad A. Alatawi, Muneefah Abdullah Alenezi, Fauzeya M. Albalwe, Hessa Meteq R. Albalawi, Doaa Bahaa Eldin Darwish, and Eman M. Sharaf

Cite This: *ACS Omega* 2023, 8, 9969–9977

Read Online

ACCESS | Metrics & More | Article Recommendations

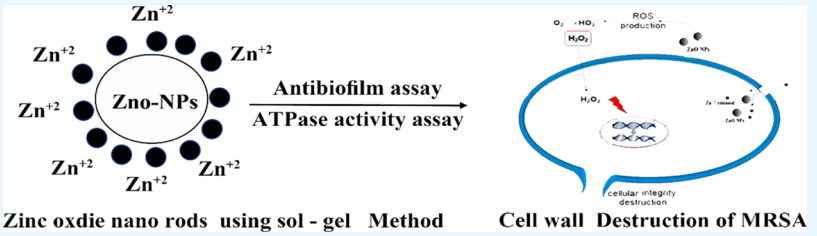

ABSTRACT: Methicillin-resistant *Staphylococcus aureus* (MRSA) causes life-threatening infections. Zinc oxide is well known as an effective antibacterial drug against many bacterial strains. We investigated the performance of zinc oxide nanorods synthesized by Albmiun as a biotemplate as an antibacterial drug in this study; the fabrication of zinc oxide nanorods was synthesized by sol−gel methods. We performed physicochemical characterization of zinc oxide nanorods by physiochemical techniques such as FTIR spectroscopy, X-ray diffraction, and TEM and investigation of their antimicrobial toxicity efficiency by MIC, ATPase activity assay, anti-biofilm activity, and kill time assays, as well as the mecA, mecR1, blaR1, blaZ, and biofilm genes (ica A, ica D, and fnb A) by using a quantitative RT-PCR assay and the penicillin-binding protein 2a (PBP2a) level of MRSA by using a Western blot. The data confirmed the fabrication of rod-shaped zinc oxide nanorods with a diameter in the range of 50 nm, which emphasized the formation of zinc oxide nanoparticles with regular shapes. The results show that zinc oxide nanorods inhibited methicillin-resistant *S. aureus* effectively. The MIC value was 23 μg/mL. The time kill of ZnO-NRs against MRSA was achieved after 2 h of incubation at 4MIC (92 μg/mL) and after 3 h of incubation at 2MIC (46 μg/mL), respectively. The lowest concentration of zinc oxide nanorods with over 75% biofilm killing in all strains tested was 32 μg/mL. Also, we examined the influence of the zinc oxide nanorods on MRSA by analyzing mecA, mecR1, blaR1, and blaZ by using a quantitative RT-PCR assay. The data obtained revealed that the presence of 2× MIC (46 μg/mL) of ZnO-NRs reduced the transcriptional levels of blaZ, blaR1, mecA, and mecR1 by 3.4-fold, 3.6-fold, 4-fold, and 3.8-fold, respectively. Furthermore, the gene expression of biofilm encoding genes (ica A, ica B, ica D, and fnb A) was tested using quantitative real-time reverse transcriptase-polymerase chain reaction (rt-PCR). The results showed that the presence of 2× MIC (46 μg/mL) of ZnO-NRs reduced the transcriptional levels of ica A, ica B, ica D, and fnb A. Also, the PBP2a level was markedly reduced after treatment with ZnO-NRs.

INTRODUCTION

MRSA is a clinical pathogen that causes infections ranging from minor skin infections to life-threatening bacteremia. Currently, the major infections are resistant to most of the antibiotics due to the formation of biofilms.[1] MRSA is the main pathogen that is isolated from surgical site infections. Many antibiotics fail to treat MRSA due to the formation of biofilms, which may lead to an increase in antibiotic resistance.[2] The formation of a slime on the synthesis surface is caused by some bacterial strains forming an adhesion biofilm.[3] Nanotechnology is a novel technological approach that involves controlling and manipulating materials in the present. Currently, nanotechnology has a central role in nanomedicine because nanostructures of different shapes have enhanced physicochemical and biological properties as well as functionalities.[4,5]

Furthermore, nanomedicine has become a vertiginous and stimulating growth area for a larger number of applications.[5,6] One-dimensional (1D) metal oxide nanostructures have been the focus of research in modern nanotechnology. There has

Received: November 5, 2022
Accepted: February 17, 2023
Published: March 6, 2023

© 2023 The Authors. Published by American Chemical Society

https://doi.org/10.1021/acsomega.2c07142
ACS Omega 2023, 8, 9969−9977

been immense interest in synthesis and application.[12] One-dimensional nanostructures such as nanorods, nanowires, nanofibers, nanobelts, and nanotubes have been a hot spot of research because of their potential technological applications.[7,8] Zinc oxide nanoparticles have a wide range of applications in the fabrication of cosmetic products such as sunblock lotion for UV protection. Because of their biocompatibility, zinc oxide nanoparticles have been approved by the Food and Drug Administration (FDA, USA).[9,10] The antimicrobial properties of zinc oxide nanoparticles depend upon liberated ROS.[11] Zinc oxide nanoparticles have better activity against pathogens as antibacterial agents, with relative safety for use in the medical field. The chemical method is thought to be an efficient way to synthesize ZnO-NPs with various chemicals, such as NaOH, but it may lead to the use of toxic chemical species as impurities in nanoparticles, which has harmed biological applications.[12] Another approach is the ecofriendly and rapid preparation of metal oxide nanomaterials like SiO_2-NPs and ZnO-NPs using natural products.[13] Additionally, other biological compounds, such as albumin and egg shell, were used to fabricate ZnO-NPs by the addition of zinc acetate to the medium in the presence of a biotemplate.[14] *Staphylococcus aureus* can form a biofilm that is encoded by ica. ADBC genes activate the synthesis of polysaccharide intracellular adhesion (PIA). PBP2 plays an important role in the survival and growth of *S. aureus*.[15] During this study, we used sol−gel techniques to prepare green zinc oxide nanorods using an albumin egg shell as a green biotemplate, and we characterized the zinc oxide nanorods using physiochemical methods. Then, we tested the antibacterial activity of ZnO-NRs, which target MRSA through ADBC genes and PBP2a protein.

MATERIALS AND METHODS

Chemicals. Zinc acetate hydrate [$Zn(CH_3COO)_2{\cdot}2H_2O$] was purchased from Oxford (India). Albumin egg shells were supplied from LOBA Chemical Co. (Mumbai, India). All solutions were prepared using ultrapure distilled water.

Synthesis of ZnO Nanorods. According to Hassan *et al.*,[3] in brief, 1.1 g of zinc acetate was added in 10 mL of ultrapure water (18 M) including 2 g of albumin and stir for 30 min until a white precipitation was formed. The white precipitation was then heated for 30 min at 70 °C before being calcined in an oven at 500 °C for 6 h, gradually annealing and characterizing.

Zinc Oxide Nanorod (ZnO NR) Characterization. The prepared ZnO-NRs were characterized by Fourier transform-infrared (FTIR) spectroscopy using Nicolet 6700 (Thermo scientific Inc., USA). X-ray diffraction (XRD) was used to elucidate the crystalline nature using a D8 Advance X-ray Diffractometer (Bruker, Germany). The size and morphology of ZnO-NRs were elucidated by using high-resolution transmission electron microscopy (HRTEM; JSM-2100F, JEOL Inc., Tokyo, Japan) at an accelerating voltage of 15 and 200 kV, respectively.

Measurement of Zn(II) Released from ZnO Nanospheres. According to Hassan *et al.* (2021), the final concentration of free zinc ions from suspended ZnO-NRs was measured using inductively coupled plasma atomic emission spectroscopy, with the following procedure: a stock solution of suspended ZnO-NRs (100 μg/mL) was diluted in PBS to a final volume of 15 mL. After that, all samples were incubated at 37 °C in a humidified atmosphere (with 5% CO_2) for various time intervals (0, 3, 6, 18, and 24 h), followed by centrifugation at 10,000*g* for 20 min and collection of a supernatant into a test tube containing 0.5 mL of conc. HNO_3. After adding up to 50 mL of water, the zinc ions were measured using an ICP-AES (Perkin-Elmer, USA).

***In Vitro* Susceptibility Test.** *Minimum Inhibitory Concentration Assay.* The standard broth microdilution method was applied to measure the minimum inhibitory concentration (MIC) of ZnO-NRs according to CLSI (2012).[18] In a 96-well microtiter plate, the bacterial inoculums were adjusted to 10^6 CFU/mL. The CLSI (2012)[18] standard broth microdilution method was used to determine the MIC of ZnO-NRs. In a 96-well microtiter plate, the bacterial inoculums were adjusted to 10^6 CFU/mL. Then, a 100 mL stock solution of ZnO-NRs (0.50−5000 μg/mL) was sonicated and inoculated with 100 μL of bacterial suspension of MRSA ATCC 33591 with a turbidity equivalent to 0.5 McFarland in the tubes, beginning from column 12 to column 3. Column 12 included the highest concentration of ZnO-NRs, while column 3 contained the lowest concentration. Column 1 included medium only, which served as a negative control. Then, a resazurin solution was added to all wells and incubated for 24 h at 37 °C. If the color changes from blue or purple to pink or colorless, it refers to bacterial growth.

Time-Kill Assay. The standard killing kinetic assay was applied according to Zhang *et al.* (2018).[18] The bacterial inoculums were adjusted in a 96-well microtiter plate to 10^6 CFU/mL. Then, ZnO-NRs were diluted with MHB media, including bacterial inoculums, to produce the following concentrations (0× MIC, 1× MIC, 2× MIC, and 4× MIC) for MRSA in a total final volume of 1 mL. The cultures were then incubated at 37 °C with 150 rpm agitation for 48 h. Then, the cultures were loaded onto MHA plates at different time intervals (0, 1, 2, 3, and 4 h). The number of colonies on the MHA plates was measured in CFU/mL after incubation for 24 h.

ATPase Activity Assay. The antibacterial activity of ZnO-NRs against *S. aureus* and MRSA was examined in the existence of the ATPase inhibitor DCCD to evaluate whether the testing material was associated with membrane function. The assay depends on the quantity of inorganic phosphate (Pi) released after adding 3 mM ATP to the membrane.[19] The method to determine Pi was described by Tausski and Shorr.[20] The bacterial strains were cultivated in the existence of ZnO-NRs (15 μg/mL). For DCCD studies, membrane vesicles were incubated with 0.3 mM DCCD for 10 min.

Anti-Biofilm Activity of ZnO-NPs. The anti-biofilm activity of ZnO-NRs was described by Kaul *et al.* (2022).[1] MRSA was diluted in a nutrient broth in a 1:100 ratio, and 100 μL of the diluted inoculum was incubated at 37 °C for 24 h on a rotating platform at 70 rpm. This was followed by washing with sterile 0.9% w/v saline to remove any planktonic bacteria. Biofilms were treated with serial dilutions of ZnO-NRs with various concentrations ranging from 1 to 128 μg/mL and further incubated at 37 °C on a rotating platform for 24 h. The bacterial viability was determined by the AlamarBlue cell viability assay after washing to discard all the testing materials.[22] Following that, 100 mL of a 10% v/v AlamarBlue (Thermo Fisher, MA, United States) solution in a nutrient broth (Thermo Fisher) was added to each well, which was then incubated at 37 °C on a rotating platform in a dark room for up to 5 h. Then, the fluorescence was measured by using a multi-scan plate reader (Thermo Fisher Scientific, USA) at

https://doi.org/10.1021/acsomega.2c07142
ACS Omega 2023, 8, 9969−9977

$\lambda_{excitation}/\lambda_{emission}$ = 530/590 nm. The biofilm inhibition percent was evaluated according to the following equation

$$\% \text{ inhibition of biofilm} = \left(1 - \frac{I_{treatment} - I_{blank}}{I_{untreated} - I_{blank}}\right) \times 100 \quad (1)$$

The antibiofilm activity of the different concentrations of ZnO-NR treatments was measured as the biofilm inhibition percentage, where $I_{treatment}$ is the intensity of treated biofilms, $I_{untreated}$ represents the intensity of untreated biofilms, and I_{blank} represents the blank intensity of the 10% v/v of the AlamarBlue solution.[22]

Reactive Oxygen Species. The reactive oxygen species (ROS) was generated by zinc oxide nanorods, which activated oxidative stress, leading to the death of the bacteria. The quantities of ROS associated with ZnO-NRs were evaluated via the detection of DCF fluorescence. The suspension of MRSA was inoculated in the zinc oxide nanorod (5, 10, and 25 μg/L) medium. After 12 h, the cells were collected and washed several times with PBS buffer. DCFH2-DA and non-treated fresh medium were added at a volume ratio of 1:2000 and incubated at 30 °C for 30 min. Then, the cells were collected by centrifugation, washed, and resuspended. The cells were immediately analyzed by flow cytometry (BD FASCCalibur-USA).[18]

Reverse Transcription-PCR. MRSA was grown in ZnO-NRs at different concentrations (1× MIC, 2× MIC, and 4× MIC) of ZnO-NRs for 30 min, while the negative control was grown without ZnO-NRs. The total RNA was prepared according to the manufacturer's procedure using a specific RNA extraction kit (Qiagen, Valencia, CA, USA). Then, the concentration of RNA was quantified by measuring A_{260} on a NanoDrop spectrophotometer (BioTek, Winooski, VT, USA). To create the RNA template for RT-PCR, we reverse-transcribed the RNA into cDNA using a cDNA synthesis kit (Qiagen, Valencia, CA, USA). The list of primer pairs that were used for the RT-qPCR is displayed in Table 1 and was designed using the NCBI primer design platform. The PCR process was then started with 10 μL of 2-SYBR premix (Life Technologies, Carlsbad, CA, USA), 2 μL of sample cDNA, 1 μL of each primer (10 μM), and 20 μL of deionized water. The PCR was run with the Step One Plus real-time PCR system (Applied Biosystems, USA).[18]

Table 1. Primers Used in Quantitative RT-PCR (qRT-PCR)

primer	sequence (5′-3′)
16S RNA	F:ACTCCTACGGGAGGCAGCAG
	R:ATTACCGCGGCTGCTGG
mecA	F:CAATGCCAAAATCTCAGGTAAAGTG
	R:AACCATCGTTACGGATTGCTTC
mecR1	F:GTGCTCGTCTCCACGTTAATTCCA
	R:GACTAACCGAAGAAGTCGTGTCAG
blaR1	F:CACTATTCTCAGAATGACTTGGT
	R:GACTAACCGAAGAAGTCGTGTCAG
blaZ	F:GCTTTAAAAGAACTTATTGAGGCTTC
	R:CCACCGATYTCKTTTATAATTT
icaA	F: ACA CTT GCT GGC GCA GTC AA
	R: TCT GGA ACC AAC ATC CAA CA
icaB	F: AGA ATC GTG AAG TAT AGA AAATT
	R: TCT AAT CTT TTT CAT GGA ATC CGT
icaD	F: ATG GTC AAG CCC AGA CAG AG
	R: AGT ATT TTC AAT GTT TAA AGCAA
fnbA	F: CAT AAA TTG GGA GCA GCA TCA
	R: ATC AGC AGC TGA ATT CCC ATT

Western Blot Analysis. MRSA was grown in ZnO-NRs at different concentrations (1/8 percent MIC, 1/4 MIC, and 1/2 MIC) for 30 min, while the negative control was grown without ZnO-NRs. The collected bacterial proteins were extracted and suspended in an extraction kit (iNtRON iotechnology), including Tris-HCI (pH 7.5). According to the manufacturer's procedure, we used a Bio-Rad protein assay reagent (Bio-Rad Laboratories, Hercules, CA, USA) to elute the protein concentrations. As a result, the supernatant was collected, and aliquots of protein in equal amounts were placed in new tubes. SDS-PAGE was used to separate proteins, which were then transferred onto nitrocellulose membranes (Millipore, MA, USA) for 3 h at 250 mA at 4 °C using the Bio-Rad electroblotting system (Bio-Rad Mini Trans-Blot Electrophoretic Transfer Cell). We used 5% skim milk in Tris-buffered saline with Tween-20 buffer to block the membrane. After blocking, the membranes were probed with monoclonal mouse anti-PBP2a primary antibody and GPDH (diluted 1:1000, Bio-Rad, USA) and re-probed with an anti-mouse IgG secondary antibody (diluted 1:2000, Enzo Life Sciences, Ann Arbor, MI, USA). Then, the membranes were treated with ECL PrimeWestern Blotting Detection Reagent (Invitrogen, USA), and the bands were visualized with an Image Quant LAS-4000 mini chemical luminescent imager (GE Healthcare Life Sciences).[23]

Statistical Analysis. In this work, the experiments were carried out in triplicate as independent experiments, and the mean and standard deviation of the independent triplicate experiments were calculated. Two sample comparisons of means were carried out using Student's *t*-test analysis. All analyses were conducted using SPSS 17.0 software (SPSS Inc., Chicago, IL, USA). A statistically significant difference was defined as $P < 0.05$.

RESULTS

Zinc Oxide Nanoparticle Characterization. The FTIR spectra of prepared ZnO-NRs was a result of thermal treatment of ZnO-NRs at 300 °C for 5 h. As shown in Figure 1, there was a broad band at 3604 cm^{-1} that was assigned to the OH group of the water molecule on the surface of ZnO-NRs. The band at 1601 cm^{-1} was also caused by the OH bend, which was assigned to ZnO. A strong band at 456 cm^{-1} was related to Zn−O.

XRD patterns of ZnO-NRs are shown in Figure 2. Peaks at 2θ = 31.746, 34.395, 36.226, 47.526, 56.549, 62.832, 67.893, and 69.028 were assigned to (100), (002), (101), (110), (103), (200), (112), and (201) of ZnO nanoparticles. All of the peaks agreed with a hexagon Wurtzite structure (Zincite, JCPDS no.: 89-0510). No characteristic peaks of any impurities were detected, referring to the high quality of ZnO-NRs.

The morphology and shape of ZnO-NRs were elucidated using TEM. As shown in Figure 3, the TEM image illustrated the rod, and its size was estimated at 50 nm and length at 200 nm, which emphasized the formation of ZnO-NRs with regular shapes as displayed in Figure 3.

Measurement of Zn(II) Released from ZnO Nanospheres. The measurement of Zn^{2+} ions liberated in the supernatant of the dispersed ZnO nanospheres (100 mg/mL) was carried out by ICP-AES. The quantitative amount of free

https://doi.org/10.1021/acsomega.2c07142
ACS Omega 2023, 8, 9969−9977

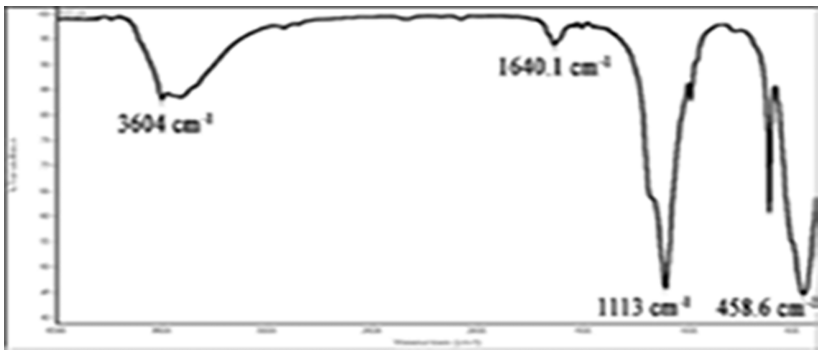

Figure 1. FTIR image of zinc oxide nanorods.

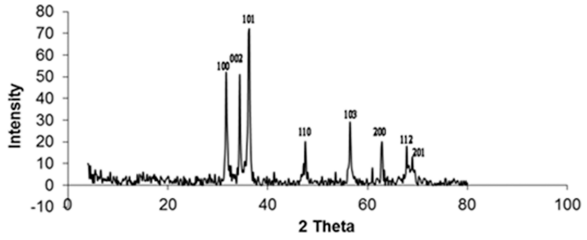

Figure 2. XRD image of zinc oxide nanorods.

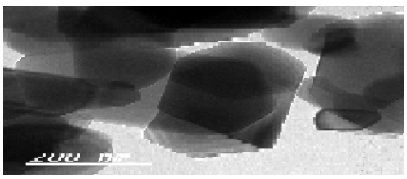

Figure 3. TEM image of zinc oxide nanorods.

Zn^{2+} varied over time intervals. The result, as shown in Figure 4, was that the liberated zinc ions were 27, 18, 10, 7.2, 3.4, and 1.1 ppm after 24, 18, 12, 6, 3, and 1 h, respectively.

Antibacterial Activity. The growth kinetic study of MRSA was carried out in the presence of zinc oxide nanorods. These studies were determined by the MIC of silver nanoparticles. They are presented in summary in Table 2 and are for MRSA. All the tested materials possessed antimicrobial activity, which is capable of inhibiting the growth kinetics of the bacterial strains. The zinc oxide nanorods had the highest effective inhibition activity against MRSA.

Table 2. Diameter MIC Value (μg/mL) for Zinc Oxide Nanorods

test material	MIC (μg/mL)
MRSA ATCC 33591	23 ± 1.09

Time-Kill Assay. The antibacterial activity of ZnO-NRs was effective against MRSA, which decreased the number of CFU/mL by 3 log units (99%) as Figure 5 shows. As shown in Figure 5, the time kill of ZnO-NRs against MRSA was achieved after 2 h of incubation at 4× MIC (92 μg/mL) and after 3 h of incubation at 2× MIC (46 μg/mL), respectively. This suggests that ZnO-NRs are effective against the MRSA bacteria strain.

ATPase Activity Assay. Figure 6 displays the activity of ZnO-NRs to reduce the ATP levels by disrupting the electrochemical proton gradient, which refers to the effect of the membrane-permeabilizing agent as well as the ATPase inhibitor on the growth of MRSA. Also, TX-100 is able to increase the permeability of the outer membrane. The viability of the bacterial strains under the combination of 30 μg/mL ZnO-NRs and 0.4 mM DCCD was reduced by 33.3 for MRSA. As compared with the OD 600 value of 30 μg/mL ZnO-NRs alone, the value of OD 600 of the suspension including 30 μg/mL ZnO-NRs with 0.00001% TX-100 was reduced by 50% for MRSA. Finally, ZnO-NRs are a great bactericide for MRSA because they are able to affect the ATPase. Also, ATPase

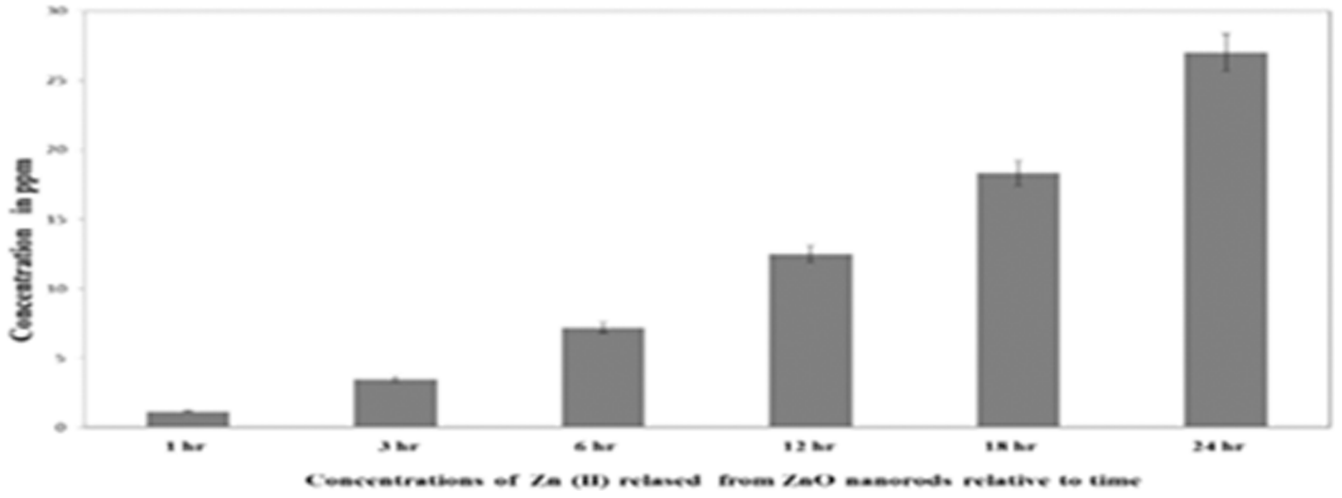

Figure 4. Released Zn^{2+} ions from ZnO nanospheres by ICP-AES.

https://doi.org/10.1021/acsomega.2c07142
ACS Omega 2023, 8, 9969−9977

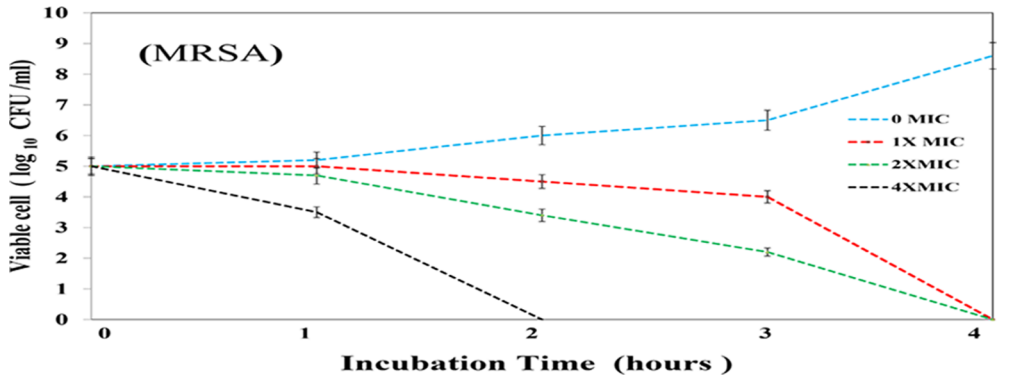

Figure 5. Time-kill assay of zinc oxide nanorods against MRSA.

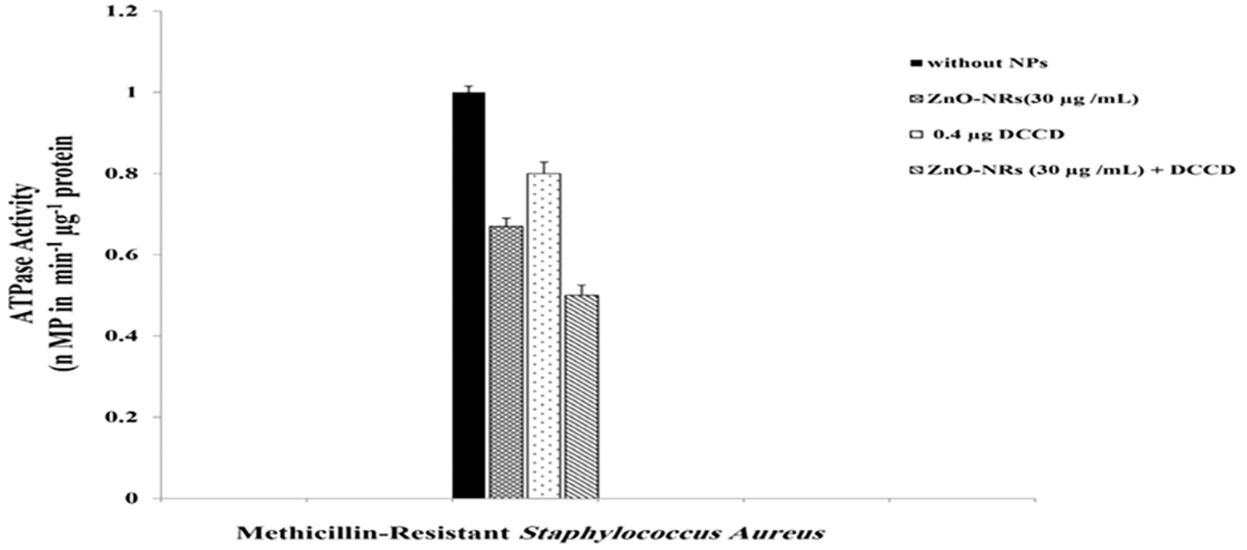

Figure 6. ATPase assay of zinc oxide nanorods against MRSA.

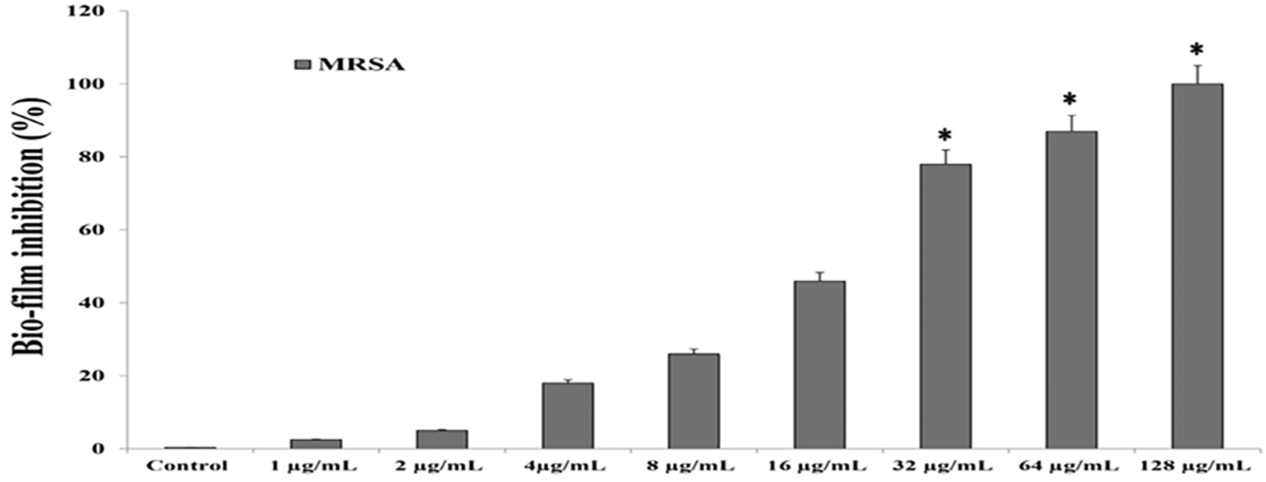

Figure 7. Anti-biofilm assay of zinc oxide nanorods against MRSA.

activity was changed in the absence of an inhibitor such as DCCD, an H+-translocator.

Effect of Different ZnO-NR Concentrations on MRSA Biofilms. MRSA biofilms were exposed to combined treatments of ZnO-NRs (1 to 128 μg/mL). In Figure 7, the MRSA biofilm killing of different ZnO-NRs was compared to the non-treatment. Overall, treatment with ZnO-NR concentrations below 8 μg/mL resulted in low antibiofilm activity against MRSA with less than 26% biofilm killing; the highest biofilm killing was 87 and 100%, $p \leq 0.001$ with 64 and 128 μg/mL ZnO-NRs for MRSA, respectively. The minimal concentrations of ZnO-NRs that resulted in more than 75% biofilm killing were 32 μg/mL ZnO-NRs (76% biofilm killing, $p \leq 0.001$). Complementing the results obtained against planktonic MRSA,

https://doi.org/10.1021/acsomega.2c07142
ACS Omega 2023, 8, 9969−9977

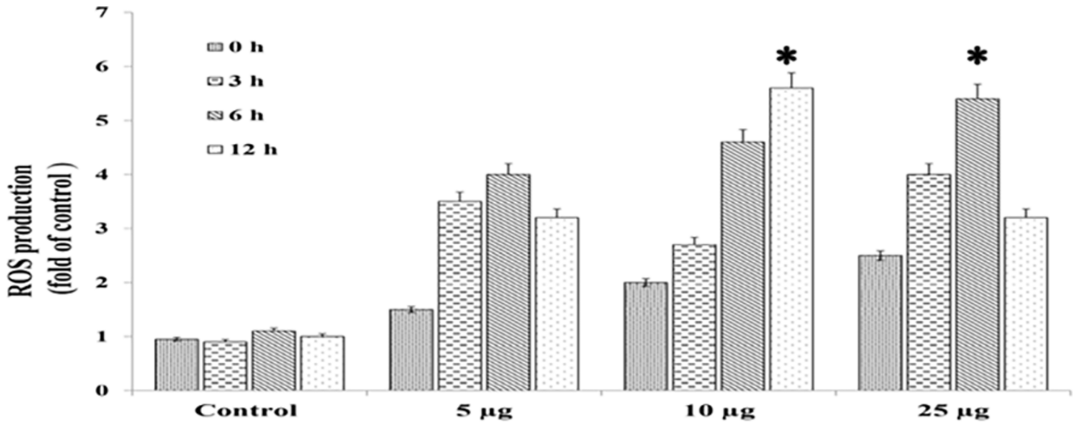

Figure 8. ROS of zinc oxide nanorods.

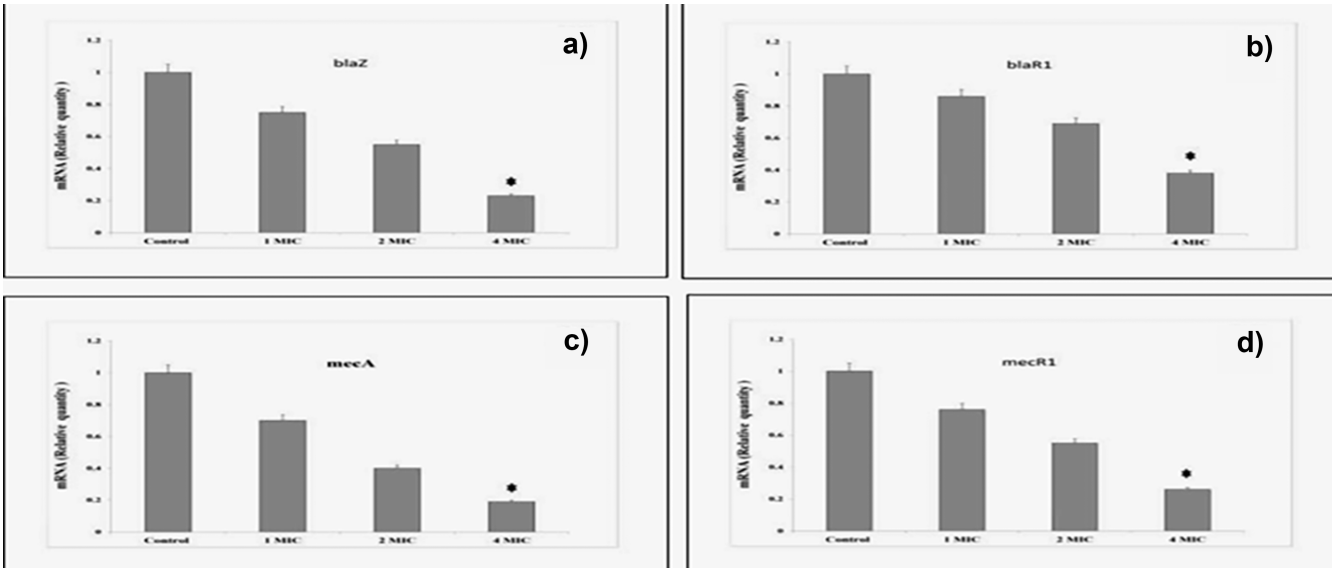

Figure 9. Rt-PCR of mecA, mecR1, blaR1, and blaZ level after treatment with ZnO-NRs.

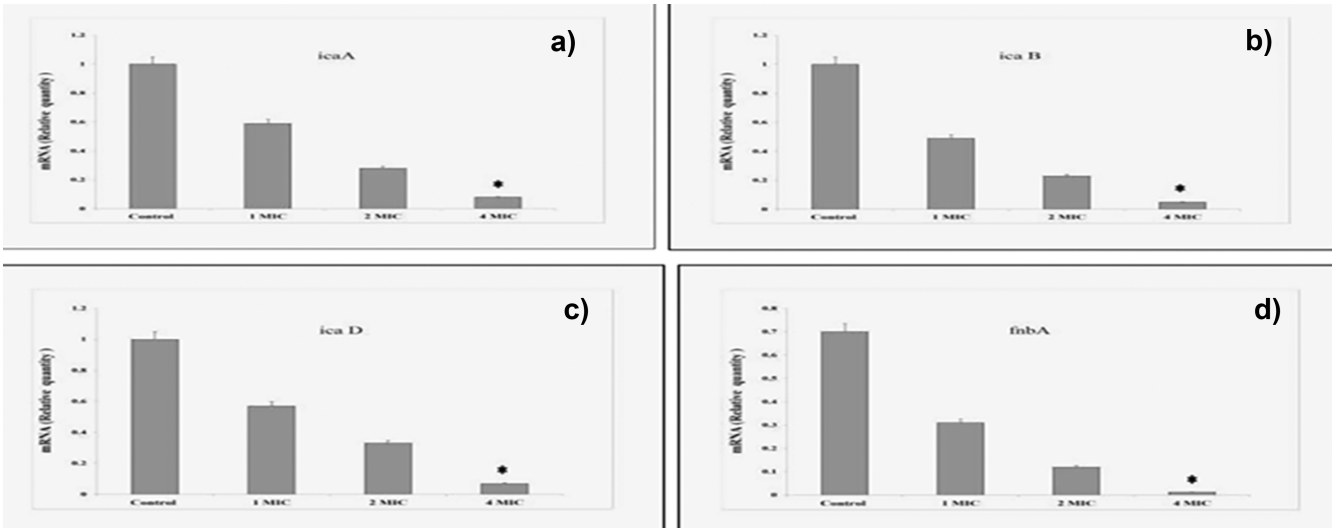

Figure 10. rt-PCR of biofilm genes (ica A, ica D, and fnb A) level after treatment with ZnO-NRs.

low antibiofilm activity was observed when ZnO-NR concentrations exceeded 16 μg/mL concentrations, suggesting the importance of a zinc oxide nanorods. The lowest concentration of zinc oxide nanorods with over 75% biofilm killing in all strains tested was 32 μg/mL. This concentration was also effective against MRSA ATCC 33591 biofilms.

https://doi.org/10.1021/acsomega.2c07142
ACS Omega 2023, 8, 9969−9977

Reactive Oxygen Species. ROS values increased as the concentrations of ZnO-NRs increased, as shown in Figure 8: ROS changed from 3.5, 4, and 3.2 at concentrations of 5 μg/mL (3, 6, and 12 h, respectively) to 4, 5.4, and 3.2 (3, 6, and 12 h, respectively) at concentrations of 25 μg/mL. The results elucidated a ZnO-NR dose-dependent increase in ROS generation in MRSA cells.[16,17,21,24]

ZnO-NRs Repress the Transcription of MecA, BlaZ, BlaR1, and MecR1 in MRSA. The transcriptional levels of blaZ, blaR1, mecA, and mecR1 were inhibited in MRSA upon treatment with 4× MIC (92 μg/mL) concentrations of ZnO-NRs, and the transcription of four genes was affected by the treatment with graded multi-inhibitory concentrations as Figure 9 shows. In the presence of 2× MIC (46 μg/mL) of ZnO-NRs, the transcriptional levels of blaZ, blaR1, mecA, and mecR1 were reduced by 3.4-fold, 3.6-fold, 4-fold, and 3.8-fold, respectively.

Furthermore, gene expression of biofilms encoding genes (ica A, ica B, ica D, and fnb A) was tested using quantitative real-time reverse transcriptase-polymerase chain reaction (rt-PCR). The results showed that due to the presence of 2× MIC (46 μg/mL) of ZnO-NRs, the transcriptional levels of ica A, ica B, ica D, and fnb A were reduced as showed in Figure 10.

Expression of PBP2a in MSRA. PBP2a expression levels under treatment with ZnO-NRs are shown in Figure 11.

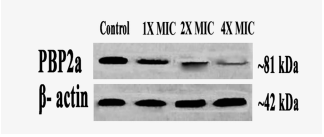

Figure 11. Western blot of penicillin-binding protein 2a (PBP2a) level of MRSA after treatment with ZnO-NRs.

Control (Lane 1), 1× MIC ZnO-NRs (Lane 2), 2× MICs (Lane 3), and 4× MIC ZnO-NRs (Lane 4) were used in the experiments. The control was not treated with ZnO-NRs. As shown in the figure, the protein level was reduced as ZnO-NRs were added at the concentrations specified, especially with 4× MIC ZnO-NRs (92 μg/mL). The PBP2a level was reduced markedly. The data indicated that the addition of ZnO-NRs reduced the PBP2a level in a dose-dependent manner.

DISCUSSION

The presence of MRSA represents nosocomial pathogens that may cause various clinical problems involving soft tissue infections, pneumonia, bacteremia, and catheter-related infections.[25] It represents a global challenge for scientists. Hence, research is ongoing to find new approaches for treating MRSA. Because MRSA is resistant to the majority of antibiotics, only a few drugs are available to patients. Methicillin-resistant *S. aureus* is resistant to all β-lactam antibiotics due to the expression of the mecA gene, which activates the encoding progression of the penicillin-binding protein 2a (PBP2a).[26,27] Currently, scientists are focusing on the development of multidrug resistance (MDR) in *S. aureus* strains. Interestingly, the formation of biofilms is a major issue because it contributes to restricting the activity of the antibiotic. It forms in *S. aureus* when encoded by the (ica) ADBC genes, which mediate the synthesis of polysaccharide intracellular adhesion (PIA).[28] Nowadays, nanomedicine has a central role in medical science applications. Over the past two decades, various metal nanoparticles have had many applications in biomedical fields such as diagnostic and therapeutic fields, anticancer therapy,[29] and antimicrobial therapy.[30] Zinc oxide's classification as an FDA-approved material depends on its properties, such as stability, safety, and intrinsic potential to neutralize UV radiation. Also, zinc oxide is used as a broad-spectrum antimicrobial.[31] The metal oxide nanostructure has been the focus of research in modern nanotechnology. One-dimensional nanostructures, including nanorods, nanowires, and nanotubes, have been the focus of research because of their potential technological applications. ZnO nanorods have a higher surface area than ZnO nanoparticles.[5] In our work, we synthesized zinc oxide nanorods using modified sol−gel by applying albumin egg shells. The explanation for the nanorod structure's formation is the accumulation of zinc ions on the surface of albumin. Then, the calcination process occurs by thermal treatment at elevated temperatures.[14] Then, we characterized the white precipitation using many techniques, such as FTIR, XRD, and TEM. The data obtained confirmed the formation of zinc oxide nanorods with a diameter of 50 nm and a length of 200 nm. Furthermore, we use MIC, ATPase activity assays, anti-biofilm activity, and kill-time assays to investigate the antimicrobial toxicity efficiency of zinc oxide nanorods. The results showed that zinc oxide nanorods had effective inhibitory activity against MRSA. The MIC value was 23 μg/mL. The time kill of ZnO-NRs against MRSA was achieved after 2 h of incubation at 4× MIC (92 μg/mL) and after 3 h of incubation at 2× MIC (46 μg/mL), respectively. The lowest concentration of zinc oxide nanorods with over 75% biofilm killing in all strains tested was 32 μg/mL. Also, we examined the influence of the zinc oxide nanorods on MRSA by analyzing mecA, mecR1, blaR1, and blaZ by using a quantitative RT-PCR assay. The data obtained revealed that the presence of 2× MIC (46 μg/mL) of ZnO-NRs reduced the transcriptional levels of blaZ, blaR1, mecA, and mecR1 by 3.4-fold, 3.6-fold, 4-fold, and 3.8-fold, respectively. Furthermore, gene expression of biofilm encoding genes (ica A, ica B, ica D, and fnb A) was tested using quantitative real-time reverse transcriptase-polymerase chain reaction (rt-PCR). The results showed that the presence of 2× MIC (46 μg/mL) of ZnO-NRs reduced the transcriptional levels of ica A, ica B, ica D, and fnb A. Also, the PBP2a level was markedly reduced, as Figure 11 shows. Interestingly, after penetrating the bacterial cell wall, zinc oxide nanorods activated the formation of free radicals, inducing the generation of ROS, which leads to spontaneous cell death (apoptosis). Also, liberated zinc ions inside the cytoplasm can generate oxidative stress, causing dispersion in membrane morphology and changing cellular architecture and intracellular biological processes, leading to cell death.[32] Finally, this study demonstrated that zinc oxide nanorods have potent anti-bacterial activity against MRSA.

CONCLUSIONS

The existence of MRSA, considered a global pathogen, may cause various clinical problems. In our work, we prepared zinc oxide nanorods using modified sol−gel by applying albumin egg shell. The formation of nanorod structures occurs by the accumulation of zinc ions on the surface of albumin, followed by thermal treatment to remove water and reshape the final structure. Many techniques were used to characterize zinc oxide nanorods, including FTIR spectroscopy, XRD, and TEM. The data obtained confirmed the formation of zinc

https://doi.org/10.1021/acsomega.2c07142
ACS Omega 2023, 8, 9969−9977

oxide nanorods with a size of 50 nm and a length of 200 nm. Also, we investigated the antimicrobial toxicity efficiency of zinc oxide nanorods by MIC, ATPase activity assay, anti-biofilm activity, and kill-time assays. In addition, we analyzed the mecA, mecR1, blaR1, blaZ, and biofilm genes (ica A, ica D, and fnb A) by using a quantitative RT-PCR assay and test transcription gene and the penicillin-binding protein 2a (PBP2a) level of MRSA using a Western blot. The data confirmed the fabrication of rod-shaped zinc oxide nanorods with a diameter in the range of 80 nm, which emphasized the formation of zinc oxide nanoparticles with regular shapes. The data show that zinc oxide nanorods have high antimicrobial activity against MRSA. The MIC of ZnO-NRs significantly reduced biofilm formation rates and the expression levels of biofilm genes (ica A, ica D, and fnb A). Furthermore, the results revealed that mecA, mecR1, blaR1, blaZ, and transcription genes, as well as the penicillin-binding protein 2a (PBP2a) level of MRSA, were significantly inhibited after being treated with ZnO-NRs.

AUTHOR INFORMATION

Corresponding Author

Amr Hassan − *Department of Bioinformatics, Genetic Engineering and Biotechnology Research Institute (GEBRI), University of Sadat City, Sadat 32897, Egypt;* orcid.org/0000-0001-6623-2179;
Email: amrhassan.nanotechnology@gmail.com

Authors

Fawziah A. AL-Salmi − *Department of Biology, Faculty of Sciences, Taif University, Taif 21944, Saudi Arabia*

Muneera A. Saleh − *Department of Biology, Faculty of Sciences, Taif University, Taif 21944, Saudi Arabia*

Jean-Marc Sabatier − *Institute de Neurophysiopathologie (INP), Aix-Marseille Université, Marseille 13005, France*

Fuad A. Alatawi − *Department of Biology, Faculty of Science, University of Tabuk, Tabuk 71421, Saudi Arabia*

Muneefah Abdullah Alenezi − *Department of Biology, Faculty of Science, University of Tabuk, Tabuk 71421, Saudi Arabia*

Fauzeya M. Albalwe − *Department of Biology, Faculty of Science, University of Tabuk, Tabuk 71421, Saudi Arabia*

Hessa Meteq R. Albalawi − *Department of Pharmacy, Prince Sultan Armed Forces Hospital, Medina 42375, Saudi Arabia*

Doaa Bahaa Eldin Darwish − *Department of Biology, Faculty of Science, University of Tabuk, Tabuk 71421, Saudi Arabia; Botany Department, Faculty of Science, Mansoura University, Mansoura 35516, Egypt*

Eman M. Sharaf − *Department of Bacteriology, Immunology, and Mycology, Animal Health Research Institute (AHRI), Shebin El Kom 11564, Egypt*

Complete contact information is available at: https://pubs.acs.org/10.1021/acsomega.2c07142

Author Contributions

Conceptualization: A.H., E.M.S., and J.-M.S.; formal analysis: E.M.S., J.-M.S., and A.H.; funding acquisition: A.H. and E.M.S.; investigation: A.H. and E.M.S.; methodology: E.M.S. and A.H.; project administration: A.H. and E.M.S.; resource: F.A.AL-S., M.A.S., F.M.A.F.A.A., M.A.A., F.M.A., H.M.R.A., and E.M.S.; supervision: E.M.S. and A.H.; validation: D.B.D.A.H. and E.M.S.; visualization: A.H. and E.M.S.; writing—original draft: A.H. and E.M.S.; writing—review edition: F.A.AL-S., M.A.S., F.M.A., H.M.R.A., and A.H.. All authors approved the final version of the manuscript.

Notes

The authors declare no competing financial interest.

The original contributions presented in the study are included in the article/Supporting Information; further inquiries can be directed to the corresponding author.

ACKNOWLEDGMENTS

The authors would like to thank the Deanship of Scientific Research at the Taif University for funding this work through Taif University Researchers Supporting Project (number TURSP—2020/113), Taif University, Taif, Saudi Arabia.

REFERENCES

(1) Kaul, L.; Abdo, A. I.; Coenye, T.; Krom, B. P.; Hoogenkamp, M. A.; Zannettino, A. C. W.; Süss, R.; Richter, K. The combination of diethyldithiocarbamate and copper ions is active against Staphylococcus aureus and Staphylococcus epidermidis biofilms in vitro and in vivo. *Front. Microbiol.* **2022**, *13*, 999893.

(2) Tong, S. Y. C.; Davis, J. S.; Eichenberger, E.; Holland, T. L.; Fowler, V. G., Jr. Staphylococcus aureus infections: epidemiology, pathophysiology, clinical manifestations, and management. *Clin. Microbiol. Rev.* **2015**, *28*, 603.

(3) Sharaf, E. M.; Hassan, A.; AL-Salmi, F. A.; Albalwe, F. M.; Albalawi, H. M. R.; Darwish, D. B.; Fayad, E. Synergistic antibacterial activity of compact silver/magnetite core-shell nanoparticles core shell against Gram-negative foodborne pathogens. *Front. Microbiol.* **2022**, *13*, 929491.

(4) Hussain, A.; Oves, M.; Alajmi, M. F.; Hussain, I.; Amir, S.; Ahmed, J.; Rehman, M. T.; El-Seedi, H. R.; Ali, I. Biogenesis of ZnO nanoparticles using Pandanus odorifer leaf extract: anticancer and antimicrobial activities. *RSC Adv.* **2019**, *9*, 15357−15369.

(5) Hassan, A.; Elebeedy, D.; Matar, E. R.; Fahmy Mohamed Elsayed, A.; Abd El Maksoud, A. I. Investigation of angiogenesis and wound healing potential mechanisms of zinc oxide nanorods. *Front. Pharmacol.* **2021**, *12*, 661217.

(6) Hassan, A.; Al-Salmi, F. A.; Abuamara, T. M. M.; Matar, E. R.; Amer, M. E.; Fayed, E. M. M.; Hablas, M. G. A.; Mohammed, T. S.; Ali, H. E.; et al. Ultrastructural analysis of zinc oxide nanospheres enhances anti-tumorefficacy against Hepatoma. *Front. Oncol.* **2022**, *12*, 933750.

(7) Zhang, Y.; Ram, K. M.; Stefanakos, K. E.; Goswami, Y. D. Synthesis, characterization, and Applications of ZnO Nanowires. *J. Nanomater.* **2012**, *624520*, 22.

(8) Yang, P.; Yan, H. .; Mao, S.; Russo, R.; Johnson, J.; Saykally, R.; Morris, N.; Pham, J.; He, R.; Choi, J. H. *Adv. Funct. Mater.* **2002**, *12*, 323.

(9) Yin, I. X.; Zhang, J.; Zhao, I. S.; Mei, M. L.; Li, Q.; Chu, C. H. The antibacterial mechanism of silver nanoparticles and its application in dentistry. *Int. J. Nanomed.* **2020**, *15*, 2555.

(10) Rauf, M. A.; Oves, M.; Rehman, F. U.; Khan, A. R.; Husain, N. Bougainvillea flower extract mediated zinc oxide's nanomaterials for antimicrobial and anticancer activity. *Biomed. Pharmacother.* **2019**, *116*, 108983.

(11) Sotiriou, G. A.; Pratsinis, S. E. Antibacterial activity of nanosilver ions and particles. *Environ. Sci. Technol.* **2010**, *44*, 5649−5654.

(12) Xu, S.; Wang, L. Z. One-Dimensional ZnO Nanostructures: Solution Growth and Functional Properties. *Nano Res.* **2011**, *4*, 1013.

(13) Sirelkhatim, A.; Mahmud, S.; Seeni, A.; Kaus, N. .H. M.; Ann, L. C.; Bakhori, S. K. M. B.; Hasan, H.; Mohamad, D. Review on Zinc Oxide Nanoparticles: Antibacterial Activity and Toxicity Mechanism. Review. *Nano-Micro Lett.* **2015**, *7*, 219−242.

(14) Nouroozi, F.; Farzaneh, F. Synthesis and Characterization of Brush-Like ZnO Nanorods using Albumen as Biotemplate. *J. Braz. Chem. Soc.* **2011**, *22*, 484−488.

(15) Tada-Oikawa, S.; Ichihara, G.; Suzuki, Y.; Izuoka, K.; Wu, W.; Yamada, Y.; et al. Zn (II) released from zinc oxide nano/micro particles suppresses vasculogenesis in human endothelial colony-forming cells. *Toxicol Rep* **2015**, *2*, 692.
(16) Loo, Y. Y.; Rukayadi, Y.; Nor-Khaizura, M. A. R.; Kuan, C. H.; Chieng, B. W.; Nishibuchi, M.; et al. In vitro antimicrobial activity of green synthesized silver nanoparticles against selected gram-negative foodborne pathogens. *Front. Microbiol.* **2018**, *9*, 1555.
(17) Andrews, J. M. Determination of minimum inhibitory concentrations. *JAntimicrob Chemother* **2001**, *48*, 5−16.
(18) Zhang, L.; Wu, L.; Si, Y.; Shu, K. Size-dependent cytotoxicity of silver nanoparticles to Azotobacter vinelandii: growth inhibition, cell injury, oxidative stress and internalization. *PLoS One* **2020**, *13*, No. e0209020.
(19) Mun, S.-H.; Kang, O.-H.; Joung, D.-K.; Kim, S.-B.; Choi, J.-G.; Shin, D.-W.; Kwon, D.-Y. In vitro anti-MRSA activity of carvone with gentamicin. *Exp. Ther. Med.* **2014**, *7*, 891−896.
(20) Blbulyan, S.; Trchounian, A. Impact of membrane-associated hydrogenases on the FoF1- bATPase in Escherichia coli during glycerol and mixed carbon fermentation: ATPase activity and its inhibition by N, N'-dicyclohexylcarbodiimide in the mutants lacking hydrogenases. *Arch. Biochem. Biophys.* **2015**, *579*, 67.
(21) Richter, K.; Ramezanpour, M.; Thomas, N.; Prestidge, C. A.; Wormald, P. J.; Vreugde, S. Mind "De GaPP": in vitro efficacy of deferiprone and gallium-protoporphyrin against Staphylococcus aureus biofilms. *Int. Forum. Allergy Rhinol.* **2016**, *6*, 737.
(22) Mun, S.-H.; Kang, O.-H.; Joung, D.-K.; Kim, S.-B.; Choi, J.-G.; Shin, D.-W.; Kwon, D.-Y. In vitro anti-MRSA activity of carvone with gentamicin. *Exp. Ther. Med.* **2014**, *7*, 891−896.
(23) Wang, S.; Kim, M. C.; Kang, O. H.; Kwon, D. Y. The mechanism of bisdemethoxycurcumin enhances conventional antibiotics against methicillin-resistant staphylococcus aureus. *Int. J. Mol. Sci.* **2020**, *21*, 7945.
(24) Zhou, T.; Li, Z.; Kang, O. H.; Mun, S. H.; Seo, Y. S.; Kong, R.; Shin, D. W.; Liu, X. Q.; Kwon, D. Y. Antimicrobial activity and synergism of ursolic acid 3-O-_-L-arabinopyranoside with oxacillin against methicillin-resistant Staphylococcus aureus. *Int. J. Mol. Med.* **2017**, *40*, 1285−1293.
(25) de San, N.; Denis, O.; Gasasira, M. F.; De Mendonça, R.; Nonhoff, C.; Struelens, M. J. Controlled evaluation of the IDI-MRSA assay for detection of colonization by methicillin-resistant, Staphylococcus aureus in diverse mucocutaneous specimens. *A J. Clin. Microbiol* **2007**, *45*, 1098−1101.
(26) Hepziba, E. R.; Soesanto, S.; Widyarman, A. S. Antibiofilm of Arumanis Mango Leaves (Mangifera indica L.) Ethanol Extract Against Staphylococcus aureus in vitro. *J. Indones. Dent. Assoc.* **2023**, *5*, 99−105.
(27) Crawford, C. L.; Dalecki, A. G.; Perez, M. D.; Schaaf, K.; Wolschendorf, F.; Kutsch, O. A copper-dependent compound restores ampicillin sensitivity in multidrug-resistant Staphylococcus aureus. *Sci. Rep.* **2020**, *10*, 8955.
(28) Fitzpatrick, F.; Humphreys, H.; O'Gara, J. P. Evidence for icaA DBC-independent biofilm development mechanism in methicillin-resistant Staphylococcus aureus clinical isolates. *J. Clin. Microbiol.* **2005**, *43*, 1973−1976.
(29) Brollo, M. E. F.; López-Ruiz, R.; Muraca, D.; Figueroa, S. J.; Pirota, K. R.; Knobel, M. Compact Ag@ Fe 3 O 4 core-shell nanoparticles by means of single-step thermal decomposition reaction. *Sci. Rep.* **2014**, *4*, 6839.
(30) Augustine, R.; Dominic, E. A.; Reju, I.; Kaimal, B.; Kalarikkal, N.; Thomas, S. Investigation of Angiogenesis and its Mechanism Using Zinc Oxide Nanoparticle-Loaded Electrospun Tissue Engineering Scaffolds. *RSC Adv.* **2014**, *4*, 51528.
(31) Zhang, Y.; Nayak, T.; Hong, H.; Cai, W. Biomedical Applications of Zinc Oxide Nanomaterials. *Cmm* **2013**, *13*, 1633.
(32) Auffan, M.; Rose, J.; Wiesner, M. R.; Bottero, J. Y. Chemical stability of metallic nanoparticles: a parameter controlling their potential cellular toxicity in vitro. *Environ. Pollut.* **2009**, *157*, 1127.

https://doi.org/10.1021/acsomega.2c07142
ACS Omega 2023, 8, 9969−9977